JOURNAL OF MATERIALS SCIENCE 18 (1983) 3571–3577

Compressive failure modes of alumina in air and physiological media

A. NASH*
Department of Metallurgy and Materials Science, Imperial College, Prince Consort Road, London, SW7, UK

Two types of α-alumina, D975 and D997, were tested under compression in air and in physiological media and the acoustic emission data recorded for each test. The typical pulse width and amplitude distributions in these tests are discussed. The scanning electron microscopy examinations showed that twinning features were encountered more frequently in the less pure material, D975, which showed a transgranular mode of fracture, while the high purity alumina had intergranular fracture surfaces. A slow rate acoustic emission, 10 to 30 events per minute, gave early warning signals of failure at about 50% failure stress, σ_f, and catastrophic failure started at above 87% σ_f. The decreased strength values are related to the surface interactions with the electrolytes in the physiological media.

1. Introduction

Alumina is considered for its use as a prosthetic material as it may overcome disadvantages inherent in materials currently in use. A general review of the early developments and the basic principles of implant selection has been given by Hastings [1]. While the metallic prosthetic components show a greater toughness, ceramic components are biologically more compatible and corrosion resistant in the body fluid [2, 3]. High purity alumina offers excellent wear properties and high compressive strength where the earlier prosthetic materials such as acrylic and Co–Cr alloy have shown abrasion of the bearing surface. On the basis of these considerations high purity alumina has gained bioengineering importance.

Microtwins have been observed in single crystals of alumina at room temperature [4]. Becher [5, 6] showed that twinning could nucleate cracks at temperatures in excess of 1200° C and at 22° C. Lankford [7] reported that shear stresses of about 500–1000 MN m^{-2} were required for twinning which nucleated transgranular microcracks.

A number of workers have studied the effect of different media on the strength of ceramics [8–11]. Braiden and Wright [12] reported significant strength reduction on bend tests of alumina in Ringer's solution at room temperature as compared to similar tests in air.

Frakes *et al.* [13] found a 35% decrease in the flexural strength of alumina aged in rabbits for 12 weeks. Ritter *et al.* [14] studied the behaviour of alumina in simulated physiological environments and concluded that such environments tend to accelerate the fatigue failure of both dense alumina and bioglass coated alumina materials although this coating appeared to act as a diffusion barrier to biological environments. Kraines and Knapp [15] found no loss of flexural strength in the case of dense alumina samples aged for 12 weeks in Ringer's solution. The porous alumina samples, however, showed a marked loss of flexural strength down to 73% of the strength before ageing in the case of samples aged for 12 weeks in Ringer's solution in an unstressed state and to 66% for those aged in a stressed condition.

Dalgleish *et al.* [16] used acoustic emission, AE, to monitor double cantilever fracture toughness tests and reported that 80% of the total number of events occurred prior to the final fracture and were associated with the subcritical crack growth. The number of emissions depended on the amount of subcritical crack growth, the grain size and the presence and the amount of porosity. Most high

*Now at Illinois Institute of Technology, METM Dept.- Rm 206 PH, 10 W 33rd St., Chicago, ILL 60616.

0022–2461/83 $03.00 + .12

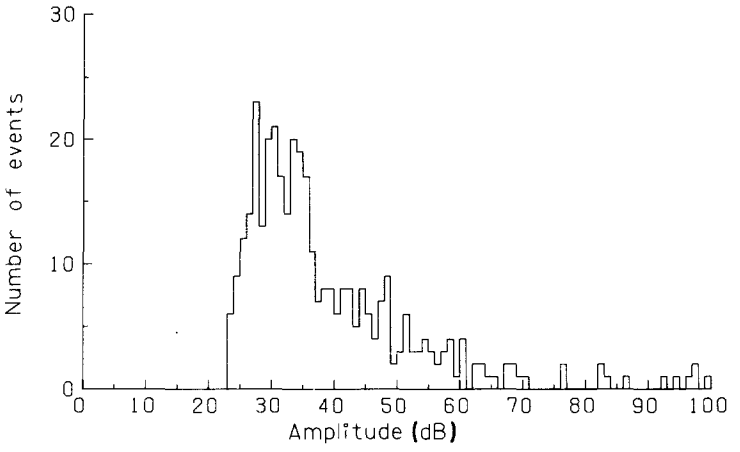

Figure 1 A typical amplitude distribution shows that the majority of events occur around 23 to 58 dB energy levels.

amplitude emissions occurred prior to failure and those occurred at the time of final fracture tended to be of high amplitude.

2. Materials and method

Two types of alpha-alumina, 97.5% and 99.7% pure designated D975 and D997, respectively, were tested in compression. The grain size in both types was a few microns with a small portion of larger grains of up to 25 microns. Rectangular polished bars were cut to 15 mm x 6 mm x 7 mm samples in the case of D975 and 15 mm^2 cross-section by 12 mm for D997 using Capco diamond wheel cutting equipment.

A steel waveguide about 50 mm long was designed consisting of a 3 mm diameter rod and two cone-shaped ends which was bonded to a sensitive transducer at one end. The waveguide-transducer bonding was maintained as a unit assembled in an environmental container surrounding the stage of a compression plate. Each sample was mounted inside the chamber longitudinally and sample-waveguide bonding was made with an adhesive. Each sample was compressed at a strain rate of $0.55 \times 10^{-3} sec^{-1}$ in an Instron testing machine following a preloading procedure to remove the relaxation and the Kaiser effect of the equipment. The transducer was connected to Dunegan/Endevco AE equipment via a preamplifier. The basic principles of equipment and the significance of the acoustic emission parameters are the same as explained elsewhere [17–19]. The compression load and the acoustic wave data were recorded by the Instron chart and a two-channel recorder connected to the equipment, respectively. At the end of the test samples generally fractured explosively into flakes, or powder. Small pieces from different tests were sputtered with gold and fracture surfaces were examined using a Cambridge scanning electron microscope (SEM) at all magnifications from 50 to 20 000. Polished surfaces of samples before and after loading to stresses up to 85% of the fracture stress were also examined. An ion beam thinning technique was used to prepare TEM samples for transmission electron microscopy.

D975 samples were tested in air and in Ringer's solution and D997 samples were tested in air, Ringer's solution, whole bovine plasma, and albumin isotonic solutions prepared in distilled water and in Ringer's solution. A minimum of 6 tests were carried out for each test condition and type of alumina.

3. Results

3.1. Acoustic emission

Linear and logarithmic distributions of pulse widths and amplitudes were plotted. The majority of events in all tests typically occurred in a range of amplitudes varying from 23 to 65 dB, Fig. 1. The AE data of all samples tested in air showed that 4% of events had amplitudes greater than 60 dB and samples tested in liquid media had up to 15% of the total number of events with amplitudes greater than 60 dB. Recording of the amplitudes was carried out in energy channels from 1 to 100 dB, a typical amplitude distribution for a given test condition may be described as a variation in the number of events likely to occur in each energy channel for those applicable, Table I. For example, D975 samples tested in air showed that the energy channels between 23 to 32 dB had

TABLE I This shows the general trend of amplitude distributions for different test conditions

Test medium and type of alumina	N_e per channel	Range of amplitudes (dB)	N_e per channel	Range of amplitudes (dB)
D975 samples				
Air	10–30	23–32	3–10	32–38
Ringer's solution	10–35	28–35	3–8	35–50
D997 samples				
Air	10–30	25–37	3–10	38–55
Plasma	10–48	27–38	3–15	38–58
Albumin in water	–	–	3–7	30–60
Albumin in Ringer's solution	–	–	3–15	30–65

recorded a minimum number of 10 events or more up to 30 events. However, for amplitude levels of 32 to 38 dB fewer events, 3 to 10, were recorded, Table I. The total number of events in the albumin solutions were reduced at the lower energy levels. The amplitudes and the number of events for tests in other liquid media were greater than those in air.

Pulse width, pw, analyser had 100 channels in 10 μsec increments in which the events were recorded, a typical distribution is shown in Fig. 2. The pulse width distributions in most tests showed a higher population of events at 70 to 120 μsec and fewer events at 120 to 1000 μsec, Table II. From this table it can be seen that D975 samples tested in air showed a greater population of events, 6 to 20, in the range of 30 to 110 μsec pw and only 2 to 10 events were recorded in each channel in the range of 120 to 500 μsec. Tests in liquid media have shown events with pw greater than 500 μsec which were not recorded for samples tested in air, Table II. Samples tested in albumin solutions showed a reduced number of events.

AE signals were first recorded at a slow rate after reaching a stress equivalent of 50% of the failure stress, σ_f, and up to the time of the catastrophic failure which occurs at or above 87% σ_f, when a rapid rate of AE took over to failure. The overlapping of signals at the catastrophic failure time is likely as microcracks developed rapidly and a great number of ringdown counts were recorded as the sound became audible. The high energy amplitudes were recorded prior to failure and during the catastrophic failure.

3.2. Microscopy

A study of SEM micrographs showed mainly transgranular fracture surfaces in D975 and intergranular failure in D997 samples, Figs. 3 and 4. All fracture surfaces showed twinning features which were also observed under the transmission electron microscope, Fig. 5. Twinning was associated with large grains and pores. SEM examination of polished surfaces did not show any twinning features in samples prior to loading and those loaded up to 50% σ_f, but samples loaded to 50 to 80% σ_f showed twinning features.

4. Discussion

Twins were found to be the main mode of defor-

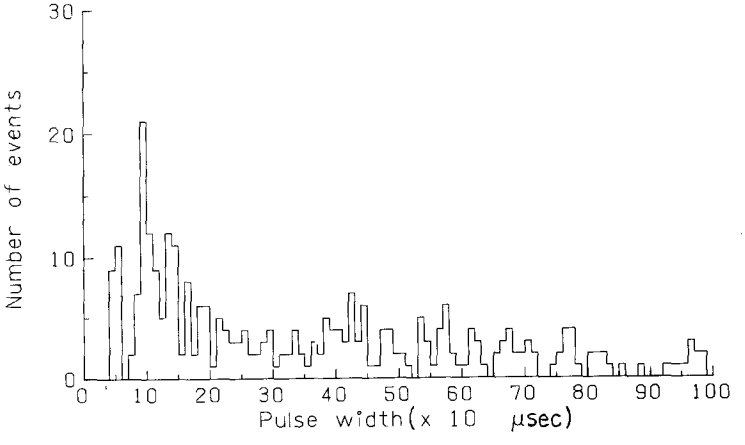

Figure 2 A typical pulse width distribution, for the same samples as in Fig. 1 shows that a higher population of events occur at 70 to 150 μsec pw and a fewer above 150 μsec.

TABLE II Shows the pulse width distribution for different test conditions

Test medium and type of alumina	N_e per channel	Range of pws (μsec)	N_e per channel	Range of pws. (μsec)
D975 samples				
Air	6–20	30–110	2–10	120–500
Ringer's solution	8–20	50–150	0–8	120–1000
D997 samples				
Air	10–36	40–120	2–10	120–400
Ringer's solution	5–25	90–120	0–10	100–1000
Plasma	8–38	70–120	0–16	120–1000
Albumin in water	0–4	70–1000	–	–
Albumin in Ringer's solution	6–14	70–110	0–4	110–1000

pw represent pulse width.

mation as can be seen from the SEM and TEM micrographs, Figs. 3 to 5. This is in agreement with the work of Lankford [7, 20] and Heuer [4]. In high purity alumina small amounts of impurity, such as silica particles, are expected to be present in the grain boundaries which act as stress raisers and induce microcracks thus causing intergranular fracture. The impurity in D975 samples was greater and twins were encountered more often than in the high purity alumina and the fracture mode was mostly transgranular. An increased impurity content in the lower purity material leads to sufficient stress raisers inside the grains which act as nucleation sites for twins. Similarly stress concentrations are caused by pores of which there was a greater population in the less pure material.

Two slopes were identified when the number of events N_e and the number of ringdown counts N_r each were plotted as a function of stress ratios with respect to the failure stress, σ/σ_f, where σ and σ_f are the stress at a given point and the fracture stress, respectively. These slopes correspond to slow and rapid acoustic emission rates which began at two stress levels, σ_1 and σ_2. About 20% of the AE occurred during the slow rate at stress levels above 50% σ_f, σ_1, and up to σ_2. 80% of the AE was

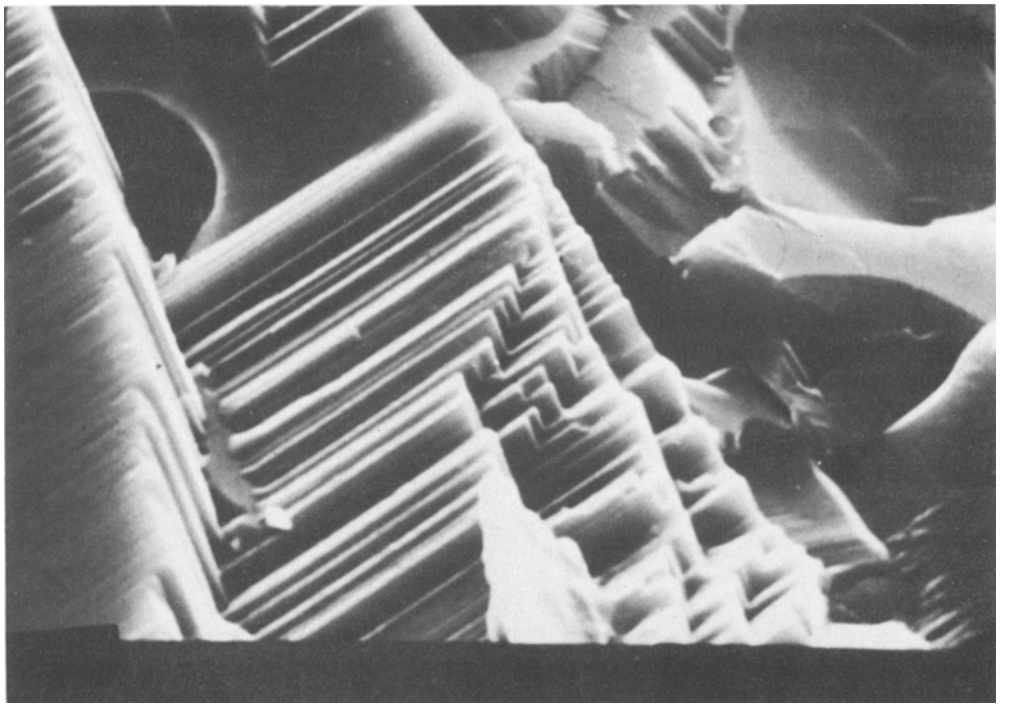

Figure 3 SEM micrograph of D975 sample showing twins associated with a pore and transgranular fracture surface. Magnification X10K, 19 mm represents 2 microns.

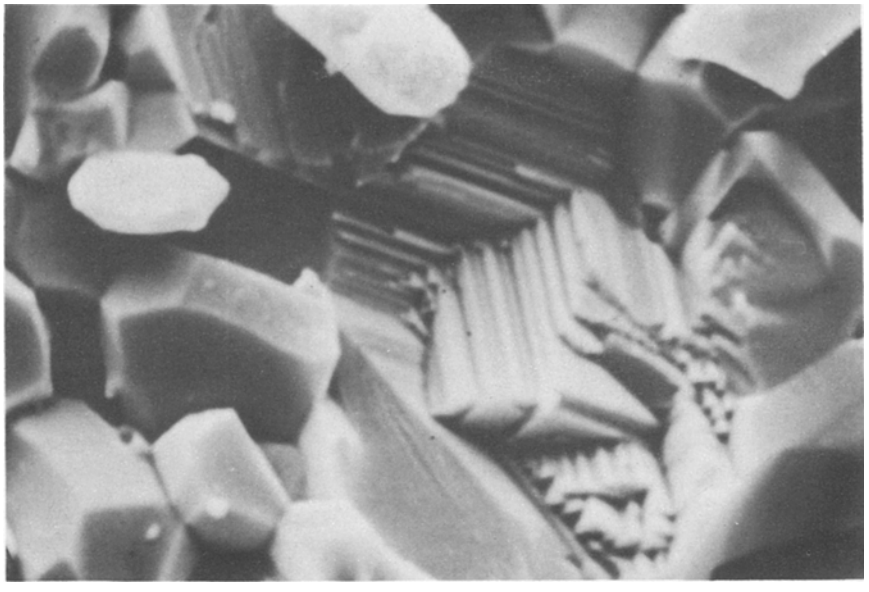

Figure 4 SEM micrograph of D997 sample at 10K magnification showing intergranular fracture surface and multiple twins. 23 mm represents 2 microns.

recorded during the catastrophic stage of the failure which occurred just prior to the total failure and was accompanied by audible crack propagation, Table III. The stress levels σ_1 and σ_2 decreased in the case of samples tested in the liquid media by 20 to 25% of the corresponding values in air. Consistent with the appearance of the AE signals deformation twinning appeared only above 50% σ_f. For alumina samples tested at a strain rate of $0.55 \times 10^{-3} sec^{-1}$ the AE data of Lankford [20] shows a threshold stress level of 53% σ_f for the formation of twins, comparable to the results in this work. The slow rate of AE may be attributed to the formation of twins in areas

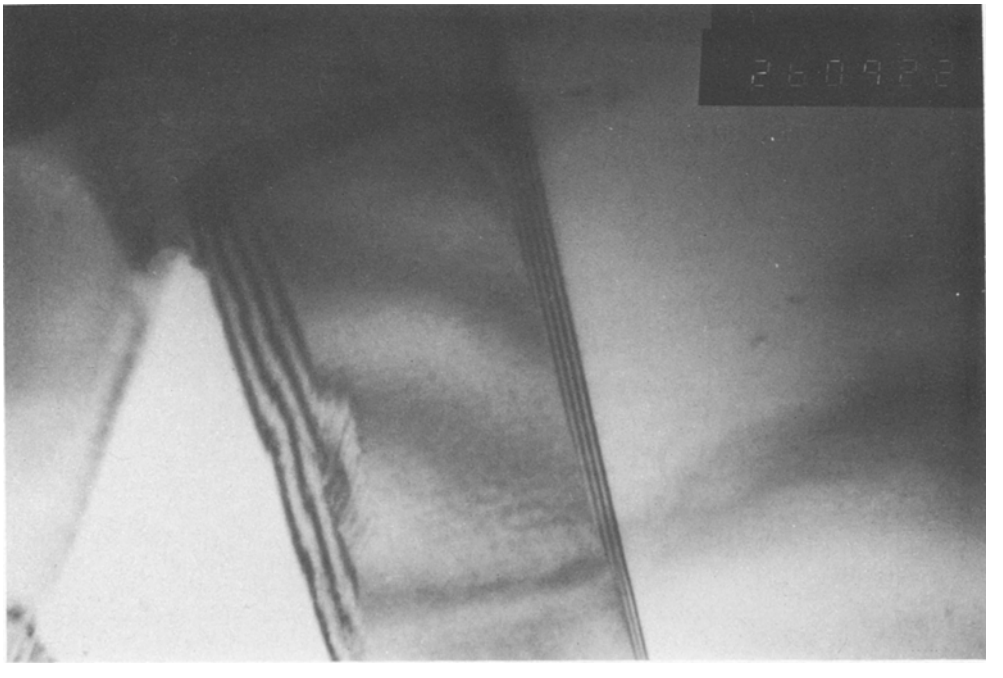

Figure 5 TEM micrograph at 260 000 magnification shows a twinning band in confirmation with the SEM results.

TABLE III The fracture strengths and the stresses at which the first and the catastrophic warning signals start are given for different test conditions

Test medium and type of alumina	Fracture stress σ_f, and SD (MN m^{-2})	σ_1, and SD (MN m^{-2})	σ_1, $\%\sigma_f$	σ_2 and SD (MN m^{-2})	σ_2, $\%\sigma_f$
D975 samples					
Air	1665, 192	950, 163	57	1450, 64	87
Ringer's solution	1160, 98	732, 91	63	1150, 107	99
D997 samples					
Air	2150, 348	1170, 190	54.4	2024, 212	94.1
Ringer's solution	1700, 206	847, 110	50	1631, 179	96
Plasma	1565, 118	965, 146	61	1529, 140	97.7
Albumin in water	1500, 75	861, 107	57.4	1414, 132	94.3
Albumin in Ringer's solution	1550, 159	944, 91	61	1528, 175	98.6

SD – standard deviation.

containing point defects and impurity particles. On increasing the load to the stress levels greater than 87% σ_f and with an increasing number of twins a rapid extension of subcritical cracks develops giving rise to an increased rate of AE and the eventual catastrophic failure. The majority of signals are therefore due to the rapid extension of subcritical cracks which were audible at stress levels above σ_2.

The concentration of dissociated water molecules in simulated physiological media is very small, pH = 7.4, however the electrical polarity of water molecules is significant and will lead to adsorption on alumina surfaces. This behaviour is important when the strength of alumina, S, is considered in relation to its surface energy, G, [21] according to

$$S = (GE/x)^{1/2}$$

where E is the Young's Modulus and x is the interatomic distance. A lowering of the surface energy leads to a decreasing strength which may occur in the case of alumina tested in physiological solution. The surface energy can be lowered as a direct result of the polar interaction of the water molecules with the surface atoms of alumina. Contact angle measurements have shown that alumina surfaces are highly wettable making an angle of 55 degrees with water [22] thus supporting the present conclusion. The lowering of the surface energy reduces the strength required to extend the microcracks on the surface which in turn lowers the overall strength, Table II.

5. Conclusion

The linear amplitude and pw distributions indicate that most signals have amplitudes varying from 23 to 60 dB and pulse widths of 70 to 120 μsec. A small portion of events have amplitudes greater than 60 dB and pulse widths longer than 120 μsec.

On loading up to σ_1 no AE signals were recorded and no twins were observed. The slow rate of AE at stress levels between σ_1 and σ_2 formed 20% of the AE and was attributed to the formation of twins. The main portion of AE, 80%, occurred at a rapid rate above $\sigma_2 \geqslant 87\% \sigma_f$ was attributed to the rapid extension of subcritical cracks.

Intergranular failure in D997 is attributed to the presence of a small amount of impurity in the grain boundaries as opposed to the transgranular mode encountered in D975 samples which is attributed to the levels of impurity inside the grains.

A substantial decrease of 20 to 25% in the strength of alumina tested in liquid media is probably due to a lowering of its surface energy as a result of the polar interactions of the water molecules with the surface atoms of alumina.

Acknowledgement

The author is grateful for the provision of a research assistantship by the Science Research Council.

References

1. G. W. HASTINGS, *J. Phys. E. Sci. Instrum.* **13** (1980) 599.
2. J. L. DRUMMOND and M. R. SIMON, in "Corrosion and Degradation of Implant Materials", edited by B. C. Syrett and A. Acharya, ASM STP 684 (Kansas City 1978).
3. P. GRISS, H. VON ADRIAN WERBURG, B. K. KREMPIEN and G. HEIMKE, *J. Biomed. Mater. Res. Symp.* **4** (1973) 453.
4. A. H. HEUER, *Phil. Mag.* **13** (1966) 379.
5. P. F. BECHER, *Mater. Sci. Res.* **5** (1971) 315.
6. *Idem, J. Amer. Ceram. Soc.* **59** (1976) 59.
7. J. LANKFORD, *J. Mater. Sci.* **12** (1977) 791.

8. J. W. DALLY, in "Studies of the Brittle Behaviour of Ceramic Materials", AFML Technical Report ASD-TR-61-628 (1963) p. 75.
9. R. J. CHARLES, in "Studies of the Brittle Behaviour of Ceramic Materials", AFML Technical Report ASD TR-61-628 (1963) p. 467.
10. W. V. BALLARD and D. E. DAY, in "Corrosion of Refractory Bond Phases of Steam–CO at 199° C", presented at Fall Meeting of the Refractories Division of the American Ceramic Society, Bedford, Pa., October 1976.
11. P. M. SINHAROY, L. L. LEVENSON, W. V. BALLARD and D. E. DAY, *Ceram. Bull.* 57 (1978) 231.
12. P. M. BRAIDEN and B. D. WRIGHT, Bioceram Symposium, Keele, September 1978 (London: Biol. Eng. Soc.).
13. J. T. FRAKES, S. D. BROWN and G. H. KENNER, *Ceram. Bull.* **43** (1974) 183.
14. J. E. RITTER, Jr, D. C. GREENSPAN, R. A. PALMER and L. L. HENCH, *J. Biomed. Mat. Res.* **13** (1979) 251.
15. F. E. KRAINES and W. J. KNAPP, *ibid.* **12** (1978) 241.
16. B. J. DALGLEISH, A. FAKHR, P. L. PRATT and R. D. RAWLINGS, *J. Mater. Sci.* **14** (1979) 2605.
17. W. SWINDLEHURST, *Non-destructive Test.* **6** (1973) 152.
18. B. J. BRINDLEY, J. Holt and I. G. PALMER, *Non-destructive Test.* 7 (1973) 299.
19. M. ARRINGTON, *Metrol Insp.* (1976).
20. J. LANKFORD, in "Fracture Mechnics of Cermics", Vol. 3 edited by R. C. Bradt, D. P. H. Hasselman and F. F. Lange (Plenum Pub. Corp., New York, 1978) p. 245.
21. R. E. REED-HILL, "Physical Metallurgical Principles" (Nostrand Co., London, 1976) p. 527.
22. S. F. HULBERT, F. M. KING, Jr, and J. J. KLAWITTER, "Bioceramics and Medical Engineering" (John Wiley and Sons Inc., London, 1971) pp. 69–89.

Received 30 November 1982
and accepted 23 March 1983